Journal of Power Sources 194 (2009) 182–189

Contents lists available at ScienceDirect

Journal of Power Sources

journal homepage: www.elsevier.com/locate/jpowsour

Compatibility of the $Py_{24}TFSI$–LiTFSI ionic liquid solution with $Li_4Ti_5O_{12}$ and $LiFePO_4$ lithium ion battery electrodes

P. Reale*, A. Fernicola, B. Scrosati

Chemistry Department, University of Rome Sapienza, 00185 Rome, Italy

ARTICLE INFO

Article history:
Received 4 March 2009
Received in revised form 11 May 2009
Accepted 12 May 2009
Available online 21 May 2009

Keywords:
Ionic liquid
Interphase
Electrochemical impedance spectroscopy
Lithium Ion battery

ABSTRACT

Ionic liquids are assuming a constantly growing importance as preferred media for the progress of various energy devices such as solar cells, supercapacitors and lithium batteries. However, their electrochemical properties are not yet fully recognized and in this paper we try to contribute to fill the gap by investigating the stability window of a sample IL-based solution, as well as its interfacial properties with two typical lithium ion battery electrodes, namely lithium titanate, $Li_4Ti_5O_{12}$ and lithium iron phosphate, $LiFePO_4$. The results of a detailed impedance spectroscopy analysis demonstrate that, although operating well within the stability domain of the selected IL-based electrolyte, both electrodes undergo passivation phenomena with the formation on their surface of a solid electrolyte interface, SEI, layer. The impedance spectra show that the resistance of the SEI is very low and stable, this suggesting that its occurrence is highly beneficial in terms of assuring reversible and safe electrode processes.

1. Introduction

Ionic liquids (ILs) are molten salts at room temperature, namely coulombic liquids. ILs have many important specific properties, including reasonably high conductivity, negligible vapor pressure, high thermal stability and non-flammability. All these properties make ILs very interesting new materials for electrochemical uses [1,2].

Among all possible applications, those directed to lithium ion batteries are highly appealing [3–5]. Indeed, the use of IL-based solutions as innovative electrolyte media contributes to overcome the safety issues associated to the evaporation, thermal instability and flammability of the organic solutions presently used in these batteries. Accordingly IL-based solutions may be the electrolytes of the future, provided that some key features, such as high lithium ion conduction and wide electrochemical stability, are met.

In principle it is not difficult to confer lithium ion transport to an IL, being it sufficient to add a suitable lithium salt [2]. However, to obtain a practically usable, IL-based, lithium ion electrolyte, certain considerations must be taken into account, in particular for what the choice of the IL itself is concerning.

Most commonly, ILs are formed of organic ions, and may undergo almost unlimited structural variations because of the easy preparation of a large variety of their components [1]. The largeness and the asymmetry of the component ions are key factors in controlling the melting temperature of a given IL, as well as in tailoring all its chemical and transport properties [1,3]. Another key aspect is the electrochemical stability domain, a parameter which rules the choice of the electrode combinations to be used in the battery.

In this latter respect, thanks to their wide electrochemical stability window, quaternary ammonium cation-based ILs are the most widely studied for electrochemical applications [4]. In particular, large attention has been addressed to imidazolium-based ILs, in virtue of their low viscosity and relatively high conductivity. Nevertheless, there are still controversial opinions on the extension of the electrochemical window of this class of ILs, especially for what the cathodic side is concerning [6–8].

Recently, we reported on a 1-*n*-butyl-1-ethyl-pyrrolidinium bis(trifluoromethane) sulfonimide IL, shortly named as $Py_{24}TFSI$, which, for battery applications, proved to be more promising than the more common imidazolium-based ILs [9]. This particular IL is characterized by a large cation with a high level of asymmetry and with a positive charge localized on the nitrogen atom, i.e. by a specific structure which, in virtue of the long alkyl chain inductive effect and of the steric hindrance, is expected to induce stabilization [10]. Analogously, the anion is large, flexible and its charge is delocalized and shielded in the inner part of the ion. All these features promote low melting temperature (−8 °C, in the case of the $Py_{24}TFSI$ IL), and high ion dissociation [11].

The synthesis, the thermal and transport properties of solutions made by dissolving a lithium salt, i.e. lithium bis(trifluoromethane)sulfonimide, LiTFSI in $Py_{24}TFSI$, were reported in a previous paper [9]. In this work we extend the electrochemical characterization of this LiTFSI–$Py_{24}TFSI$ solution,

* Corresponding author. Tel.: +39 0649913664; fax: +39 06491769.
E-mail address: priscilla.reale@uniroma1.it (P. Reale).

0378-7753/$ – see front matter © 2009 Elsevier B.V. All rights reserved.
doi:10.1016/j.jpowsour.2009.05.016

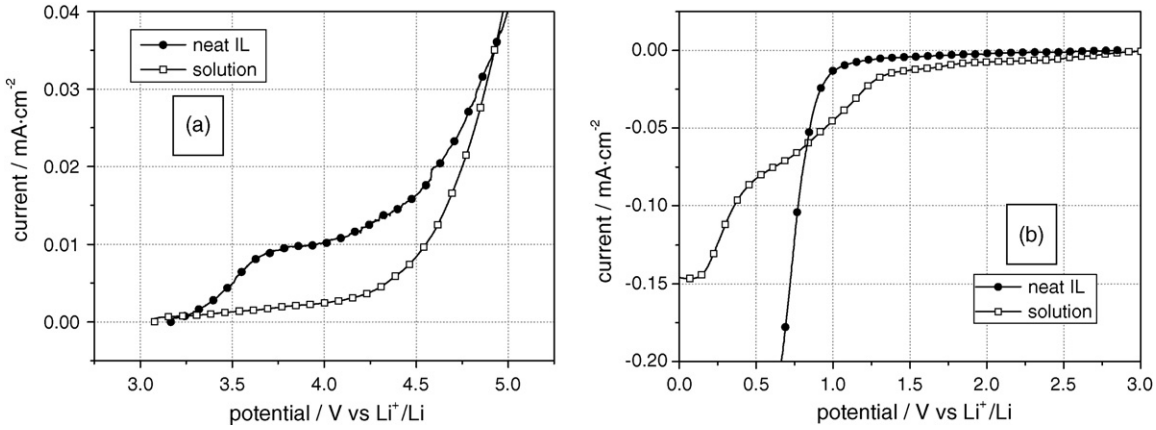

Fig. 1. Linear-sweep voltammetry of a carbon Super P electrode in the neat $Py_{24}TFSI$ ionic liquid and in the 0.2 m LiTFSI–$Py_{24}TFSI$ solution. (a) Anodic scan and (b) cathodic scan. Li counter and reference electrodes. Scan rate 0.2 mV s^{-1}.

with the main aim of clarifying the occurrence and the nature of interfacial phenomena with electrodes of interest for lithium ion battery applications. In this respect, we have focused the study on two of the most promising candidates, namely the lithium titanate $Li_4Ti_5O_{12}$ anode and the lithium iron phosphate, $LiFePO_4$ cathode.

2. Experimental

The $Py_{24}TFSI$ ionic liquid and its 0.2 m LiTFSI–$Py_{24}TFSI$ solution were prepared according to the procedure reported in reference [9]. Lithium titanium oxide was obtained through a solid-state synthesis, by annealing under oxygen flux an intimate mixture of stoichiometric amount of $LiOH{\cdot}H_2O$ (Aldrich 98%) and TiO_2 anatase (Aldrich 99.9%) at 800 °C for 12 h [12]. Lithium iron olivine was prepared by calcinating under nitrogen flux a stoichiometric mixture of Fe^{II} phosphate and lithium phosphate at 700 °C for 12 h [13]. The precursor was synthesized by a low-cost aqueous precipitation technique described elsewhere.

Electrode films were obtained by casting onto an Al foil a mixture of 80% active material ($Li_4Ti_5O_{12}$ and $LiFePO_4$, respectively), 10% Super P carbon and 10% poly(vinylidenfluoride), PVdF dissolved in *n*-methylpyrrolidinone.

The electrochemical stability windows of the neat IL and of the 0.2 m LiTFSI–$Py_{24}TFSI$ solution, respectively, were determined by linear-sweep voltammetry of a Super P carbon working electrode run at 0.2 mV s^{-1} in a three-electrode cell having a Super P carbon working electrode and lithium foil as reference and counter electrode. The test was performed by using a PAR 362 potentiostat.

The cyclic voltammetry of the $Li_4Ti_5O_{12}$ and $LiFePO_4$ electrodes in the 0.2 m LiTFSI–$Py_{24}TFSI$ solution was run at 0.2 mV s^{-1} and at 40 °C using a PAR 362 potentiostat. The galvanostatic charge–discharge tests were performed at a C/10 rate (i.e. 1 lithium equivalent in 10 h) using a Maccor 8000 Battery Tester system.

The characteristic of the $Li_4Ti_5O_{12}$/0.2 m LiTFSI–$Py_{24}TFSI$ interface and of the $LiFePO_4$/LiTFSI–$Py_{24}TFSI$ interface were investigated by impedance spectroscopy run on various types of cell, namely (i) three-electrode cells using lithium counter and lithium reference electrodes, (ii) symmetrical two-electrode cells using two twins electrodes (i.e. two $Li_4Ti_5O_{12}$ electrodes or, in alternative, two $LiFePO_4$ electrodes) and (iii) three-electrode cells using two twins electrodes (i.e. two $Li_4Ti_5O_{12}$ electrodes or, in alternative, two $LiFePO_4$ electrodes) in connection with a third, lithium sink electrode (i.e. $LiFePO_4$ or, in alternative, $Li_4Ti_5O_{12}$) of a different kind (for details see below). The related impedance spectra were obtained by a Solartron Frequency Response analyzer in a 0.01–100 kHz frequency range. Impedance deconvolution and non linear least square refinement have been performed by mean of the EQUIVCRT software by Boukamp [14].

3. Results and discussion

The characterization of the 0.2 m LiTFSI–$Py_{24}TFSI$ solution was first directed to the investigation of its stability window. This is an important parameter since it allows defining the voltage range of applicability of the electrolyte. Typically, this evaluation is performed by running a sweep voltammetry on a working, here Super P carbon, electrode placed in the solution under test, here the 0.2 m LiTFSI–$Py_{24}TFSI$ solution. The onset of the current in the cathodic and in the anodic side gives the decomposition voltages which set the limits of the stability window of the electrolyte. Clearly, under these practical conditions, the extension of the stability window is a function of the nature of the working electrode. We have used a large surface area carbon electrode on which the decomposition reactions are expected to be particularly enhanced. This most unfavourable case was chosen on purpose in order to be sure that the limits set by this electrode may hold for any other alternative electrode material. The choice was also motivated by the fact that carbon is present in all electrode configurations of practical lithium batteries and thus, its use as testing electrode may well mimic the real conditions.

Fig. 1 reports the results of the stability test in terms of current–voltage curves of the C working electrode. Fig. 1a compares the anodic scans obtained in a cell using the neat $Py_{24}TFSI$ ionic liquid and the 0.2 m LiTFSI–$Py_{24}TFSI$ solution, respectively. Clearly, the addition of LiTFSI largely improves the anodic stability which passes from about 3.5 V vs. Li to more than 4.5 V vs. Li. This result has important implications since it demonstrates that the solution may be safely used in connection with high voltage cathodes. The reason why the lithium salt is capable to extend the anodic electrochemical stability is not yet totally clear. Quite likely, the effect is associated to specific interactions between the salt and the ionic liquid, which result in the enforcement of the overall structure. Spectroscopic investigation is under way to confirm this hypothesis.

Fig. 1b shows the stability response in the cathodic side. In this case the addition of the lithium salt is not fruitful, but rather deleterious since it anticipates the onset of the current to a decomposition value of 1.5 V vs. Li in respect to that experienced with the neat ionic liquid, i.e. 0.8 V vs. Li. However, we notice from Fig. 1b that the current profile related to the cell using the solution reveals a second process at about 0.3 V vs. Li. This strongly suggests that the first decomposition process at 1.5 V results in the formation of a solid electrolyte interface (SEI), passivating film on the electrode surface which kinetically extends the stability down to 0.3 V.

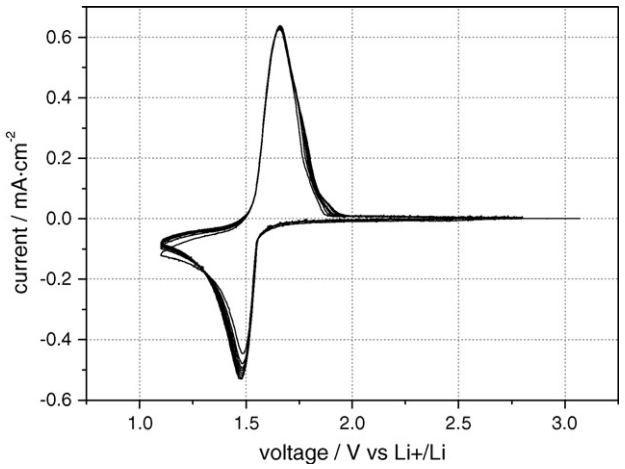

Fig. 2. Cyclic voltammetry at 40 °C of a $Li_4Ti_5O_{12}$ electrode in a 0.2 m LiTFSI–Py_{24}TFSI solution. Li counter and reference electrodes. Scan rate: 0.2 mV s^{-1}.

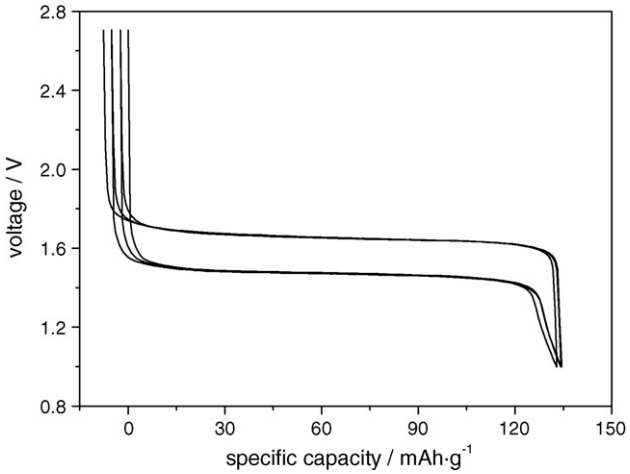

Fig. 3. Galvanostatic voltage profile of the Li insertion–Li deinsertion cycles of a $Li_4Ti_5O_{12}$ electrode in a 0.2 m LiTFSI–Py_{24}TFSI solution at 40 °C. Li counter. Current rate: C/10.

In view of the above considerations, we may assume for the 0.2 m LiTFSI–Py_{24}TFSI solution a stability window ranging from 1.4 to 4.6 V, with a possible extension to lower cathodic voltages due to the formation of a protective SEI. Therefore, in terms of lithium ion battery applications, the 0.2 m LiTFSI–Py_{24}TFSI solution is compatible with the majority of common positive electrodes (cathodes), e.g., $LiCoO_2$, $LiMn_{0.5}Ni_{0.5}O_2$, $LiCo_{0.33}Mn_{0.33}Ni_{0.33}O_2$, $LiFePO_4$, while the use of negative electrodes (anodes) appears to be preferable for materials operating within the 1.5 V range, although, due to the protection of the SEI layer, extension to lower voltage anodes cannot be excluded.

On the basis of the above considerations, we concentrated our study to electrode combinations based on a $Li_4Ti_5O_{12}$ anode and a $LiFePO_4$ cathode, both operating within the stability window of the 0.2 m LiTFSI–Py_{24}TFSI solution, namely 1.5 V vs. Li for the former and 3.5 V vs. Li for the latter. To be noticed that the $Li_4Ti_5O_{12}$–$LiFePO_4$ system has been successfully used in lithium ion batteries using conventional liquid electrolytes [15]. Indeed, results originally obtained in our laboratory [15] and later confirmed by many other authors have demonstrated that this electrode combination gives a ~2 V battery with excellent performances in terms of reliability and cycle life.

It is then expected that this combination may also be highly beneficial for developing efficient ionic liquid battery systems. To confirm this, it has appeared to us of interest to explore the electrochemical behaviour of both the $Li_4Ti_5O_{12}$ and $LiFePO_4$ electrodes, by focusing on their kinetic and interfacial properties when in contact with our 0.2 m LiTFSI–Py_{24}TFSI solution.

3.1. Properties of the $Li_4Ti_5O_{12}$ electrode in the IL-based electrolyte

Fig. 2 shows the cyclic voltammetry of the $Li_4Ti_5O_{12}$ electrode at 40 °C. The voltammetry develops with well reproduced peaks, centred around 1.48 V vs. Li, and around 1.66 V vs. Li, representing the well-known, Li insertion Li deinsertion, electrochemical process:

$$Li_4Ti_5O_{12} + Li \leftrightarrows Li_7Ti_5O_{12} \quad (1)$$

to which is associated a theoretical specific capacity of 175 mAh g^{-1}. The shape of the voltammetry curves confirms that the electrode maintains high reversibility and fast kinetics also in the ionic liquid medium.

The good behaviour of the lithium titanate electrode is also demonstrated by the trend of its typical Li insertion–Li deinsertion cycles, reported in Fig. 3. As typically expected for the two-phase process [1], the voltage profiles are flat and the capacity is quite high, i.e. close to the 80% of the theoretical value. We may then conclude that the $Li_4Ti_5O_{12}$ electrode behaves in the IL-based solution as well as in the common organic electrolytes. To be noticed in this respect that, while the main electrochemical process of the $Li_4Ti_5O_{12}$ electrode develops within the stability domain of the electrolyte, the cathodic cut-off potential is at its limit. Nevertheless, Figs. 2 and 3 demonstrate that the electrode cycles well with no sign of deterioration. This may be explained on the basis of the proposed extended stability promoted by the SEI formation, see Fig. 1b and related discussion. In alternative, difference in kinetic stability passing from a Super P electrode (Fig. 1b) to $Li_4Ti_5O_{12}$ electrode, where the amount of Super P is much less, cannot be excluded.

To confirm this explanation, we have carried out a detailed impedance analysis of the $Li_4Ti_5O_{12}$ electrode in the 0.2 m LiTFSI–Py_{24}TFSI solution. The idea was to investigate the condition of the interface with the main aim of detecting the eventual occurrence of side reactions and finally, of demonstrating the formation of the SEI. For this test we have used a three-electrode cell, equipped with lithium counter and lithium reference electrodes, in order to evidence the response of the single $Li_4Ti_5O_{12}$ electrode under different operating conditions.

Fig. 4a shows a series of impedance plots collected at various stages of the electrochemical process of the $Li_4Ti_5O_{12}$ electrode in the 0.2 m LiTFSI–Py_{24}TFSI solution, namely in its pristine state, in the full discharge (Li intercalation) stage (1.2 V vs. Li), after three full cycles, in the half discharge state at 1.6 V vs. Li in the plateau (compare Fig. 3) and finally, to evaluate aging effects, after 25 full cycles. The first evidence is that the impedance responses evolve without signs of major deterioration. In the pristine state and whenever the electrode is cycled and left in its charged state, the main feature of the spectra is a capacitive trend at low frequency, as typical for an electrode in its blocking state. The absence of deviation from this expected trend excludes the occurrence of side reactions with the electrolyte. The electrode becomes non-blocking when $Li_4Ti_5O_{12}$ is in equilibrium with $Li_7Ti_5O_{12}$ (see [1]), i.e. at 1.6 V vs. Li. By zooming the high frequency region (see inset of Fig. 4a), it is possible to detect the convolution of at least two semicircles. Considering the frequency and capacitance values, it is possible to attribute this multi-semicircle response to the presence of a multilayer SEI.

The overall spectra was then fitted with an equivalent circuit composed of a series of three parallel RQ elements, see Fig. 4c. The fitting analysis suggested an interpretation based on the sequence of two high frequency semicircles (associated to the formation

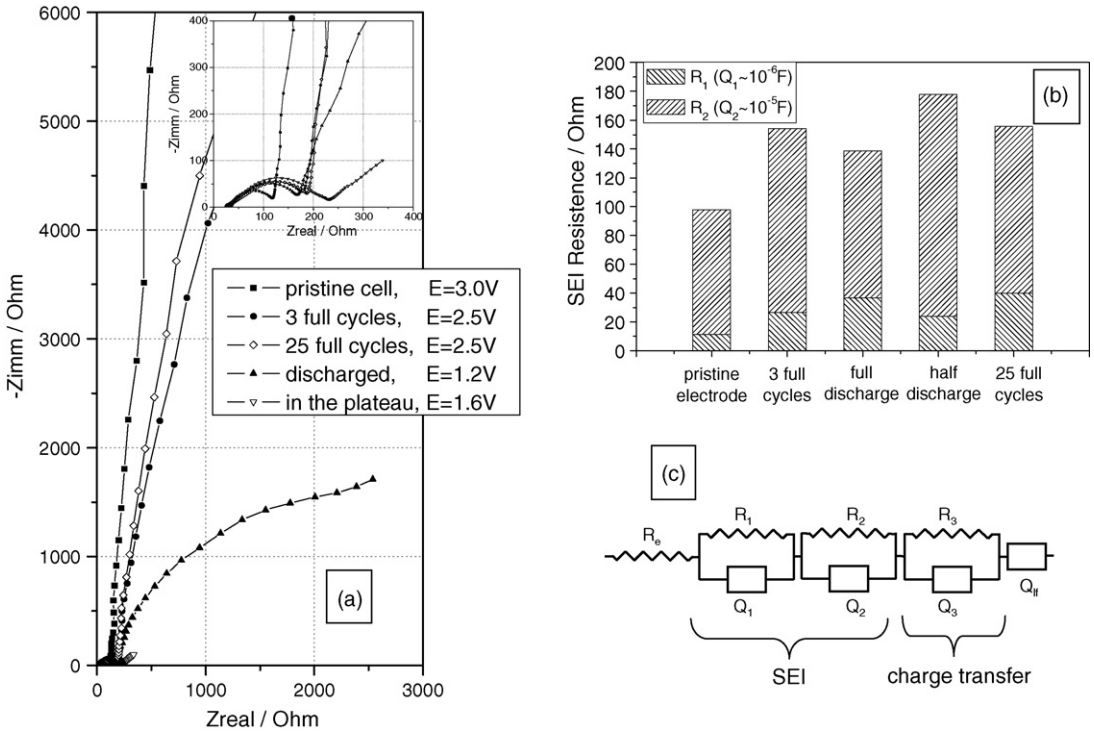

Fig. 4. Impedance response of a $Li_4Ti_5O_{12}$ electrode in a 0.2 m LiTFSI–Py_{24}TFSI solution under various stages of the electrochemical process. (a) Nyquist plots; (b) values of the interface resistance; (c) equivalent circuit. Li counter and reference electrodes.

of a passivating film), followed by a middle frequency semicircle (associated to the charge transfer) and finally, by a geometric capacitance. This appears as a good evidence of the SEI occurrence on the electrode surface, also supported by the fact that its overall interfacial resistance, after an initial growth, stabilizes around a low 150 Ω value, see Fig. 4b.

However, under the experimental conditions used for the test, one cannot rule out that the origin of the SEI on the $Li_4Ti_5O_{12}$ surface, rather than being solely an intrinsic feature of the electrode, may be due to the precipitation of decomposition products formed onto the surface of the lithium counter electrode. To exclude this possible interference, we designed two additional tests. In the first

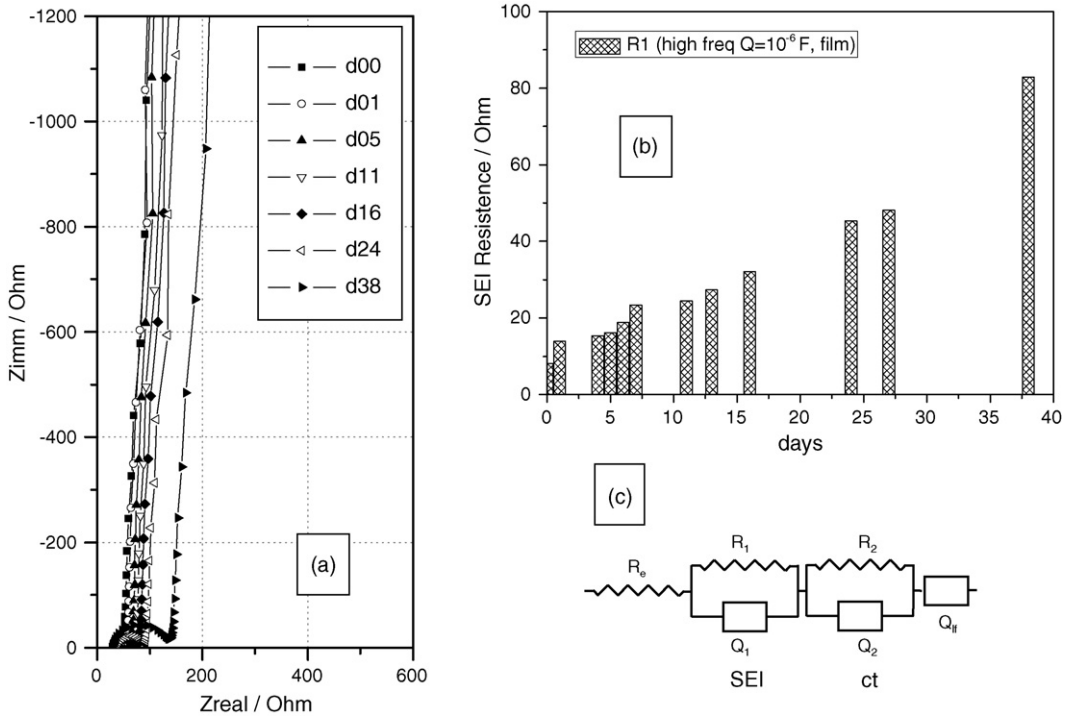

Fig. 5. Impedance response of a symmetrical, lithium-free cell formed by two twin $Li_4Ti_5O_{12}$ electrodes in their charged state, i.e. at ~3 V vs. Li, in a 0.2 m LiTFSI–Py_{24}TFSI solution. (a) Nyquist plots at various storage times: d00 means on assembly, d01 means after 1 day, d05 after 5 days and so on; (b) time evolution of the interface resistance; (c) equivalent circuit.

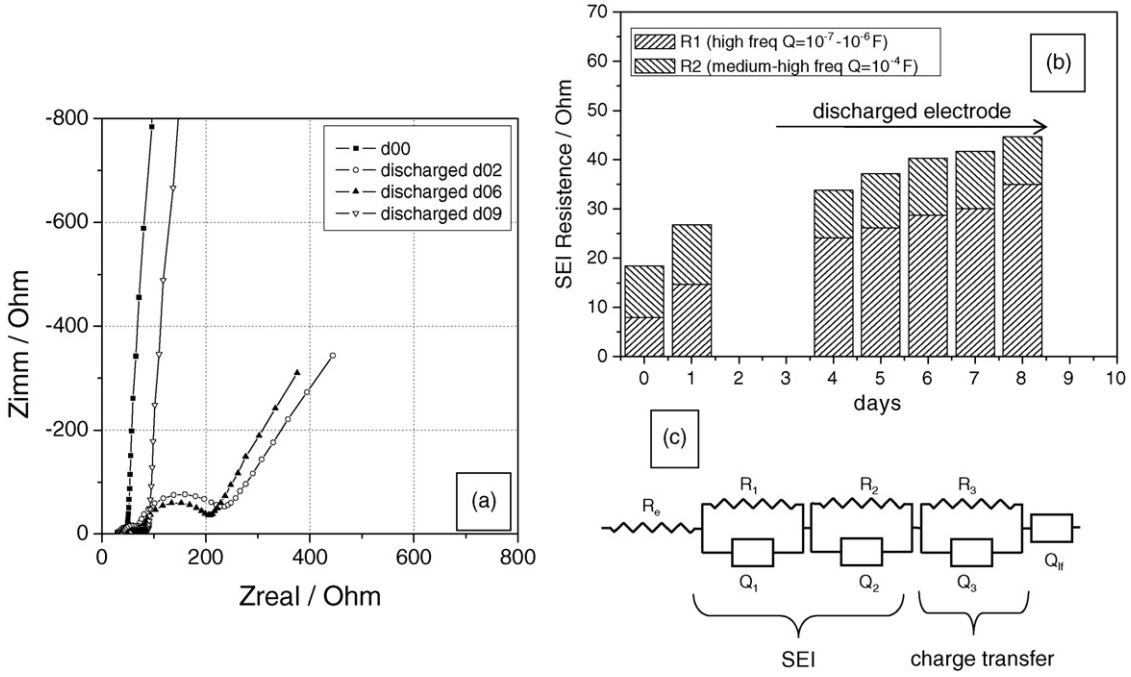

Fig. 6. Impedance response of a symmetrical, lithium-free cell formed by two twin $Li_4Ti_5O_{12}$ electrodes plus a third, lithium sink $LiFePO_4$ electrode, in a 0.2 m LiTFSI–Py_{24}TFSI solution. (a) Nyquist plots in the pristine state and after half-discharge; (b) time evolution of the interface resistance; (c) equivalent circuit.

one, we run an impedance analysis on a symmetrical cell formed by two $Li_4Ti_5O_{12}$ twin electrodes, both in their charged state, i.e. at ~3 V vs. Li. The response of this, totally lithium-free, cell is shown in Fig. 5a. The data were obtained at a progressive storage time extended to a total of 38 days. No electrochemical reaction is possible for the cell under test since formed by two fully oxidized, equal electrodes and, accordingly, the general trend of the impedance response is that associable to a blocking system. However, a closer look at the spectra reveals the occurrence of a series of events. These can be described by a semicircle developing at high frequency, which can be ascribed to the presence of a SEI, followed by another semicircle in frequency region where phenomena related to charge transfer, i.e. ion desolvation/adsorption are generally detected. Therefore, these results tend to suggest that a SEI is formed on the $Li_4Ti_5O_{12}$ electrodes even when they are in their charged state, namely well within the stability domain of the electrolyte. It is difficult to rationalize the SEI formation under these voltage conditions; one can only assume that it may be due to a reaction with some residual impurities in the electrolyte. However, the important fact in relation to possible battery applications, is that the resistance of the SEI is comparably quite low and increases very slowly upon time of storage, see Fig. 5b, this finally demonstrating the excellent stability of the $Li_4Ti_5O_{12}$/0.2 m LiTFSI–Py_{24}TFSI solution interface.

A second $Li_4Ti_5O_{12}$/$Li_4Ti_5O_{12}$ cell was assembled, however with the addition of a third electrode. The latter was $LiFePO_4$ and its role was to deliver lithium to the two $Li_4Ti_5O_{12}$ electrodes in order to bring them to their half discharged (i.e. lithium inserted) state, thus avoiding the use of metal lithium in the cell. The two $Li_4Ti_5O_{12}$ electrodes were short-circuited, connected to the $LiFePO_4$ electrode and slowly discharged galvanostatically towards the half of the plateau, i.e. $Li_{5.2}Ti_5O_{12}$ (see Fig. 3). Fig. 6a shows the impedance response of the cell. As expected, when the two $Li_4Ti_5O_{12}$ electrodes are in the pristine state (i.e. before connection with the $LiFePO_4$ electrode), the response reflects their blocking behaviour. The spectra change after discharge with the evolution of two semicircles and a 45° spike indicating that interface and diffusion phenomena become relevant. However, it is very interesting to observe that, while the spectra change macroscopically upon insertion, the high frequency region (associable to the SEI) remains at very low values and almost unchanged upon time, see Fig. 6b. This is an additional, important evidence that the solid electrolyte interface on the $Li_4Ti_5O_{12}$ electrode in the 0.2 m LiTFSI–Py_{24}TFSI solution is indeed a very stable and a low resistive film.

3.2. Properties of the $LiFePO_4$ electrode in the IL-based electrolyte

The investigation of the electrode behaviour in the in the 0.2 m LiTFSI–Py_{24}TFSI solution was extended to the $LiFePO_4$ case. Fig. 7 shows the cyclic voltammetry at 40 °C. The response evidences in the very first cycle the occurrence of some irreversibility; however, the following cycles proceed with well reproduced peaks without evidence of side reactions. This behaviour is confirmed by the trend of the galvanostatic cycles, see Fig. 8, which are representative of

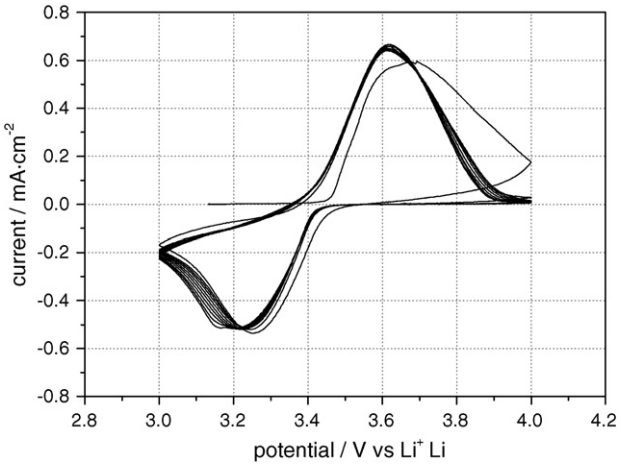

Fig. 7. Cyclic voltammetry at 40 °C of a $LiFePO_4$ electrode in a 0.2 m LiTFSI–Py_{24}TFSI solution. Li counter and reference electrodes. Scan rate: 0.2 mV s^{-1}.

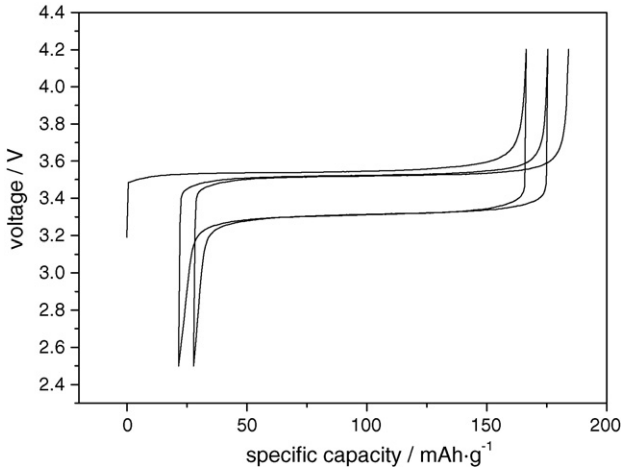

Fig. 8. Galvanostatic voltage profile of the two-phase cycling process of a $LiFePO_4$ electrode in a 0.2 m LiTFSI–Py_{24}TFSI solution at 40 °C. Li counter. Current rate: C/10.

the expected two-phase electrochemical process:

$$LiFePO_4 \leftrightarrows FePO_4 + Li \quad (2)$$

to which is associated a theoretical specific capacity of 170 mAh g^{-1}. We see that the voltage profiles evolve around 3.5 V, i.e. well within the stability domain of the electrolyte solution (compare Fig. 1a). In addition, the capacity approaches the theoretical value and thus, we may conclude that also the $LiFePO_4$ electrode behaves in the IL-based solution as well as in the common organic electrolytes.

The impedance analysis of the $LiFePO_4$ electrode in the 0.2 m LiTFSI–Py_{24}TFSI solution was carried out with a protocol similar to that used for the $Li_4Ti_5O_{12}$ electrode, with the aim of determining also in this case the conditions of the interface. Fig. 9a shows a series of impedance plots collected at various stages of the electrochemical process of the $LiFePO_4$ electrode, namely in its pristine state, in the charged ($LiFePO_4$ phase) state (4.0 V vs. Li), after three full cycles, in the half charge state (3.5 V vs. Li) in the plateau (compare Fig. 8) and finally, to evaluate aging effects, after 25 full cycles. Similar to the $Li_4Ti_5O_{12}$ case, we notice that the impedance shapes evolve without signs of major deterioration and by assuming a capacitive trend when the electrode is in its pristine state or left in its charged state. As expected, the response of the electrode becomes non-blocking in its half charged state. By zooming the high frequency region (see inset of Fig. 9a), it is possible to detect the convolution of at least two semicircles. Considering the frequency and capacitance values, the multi-semicircle response is likely associated to the presence of a multilayer SEI, see also the fitting equivalent circuit of Fig. 9c.

Therefore, also in the $LiFePO_4$ case the impedance results evidence the formation of a SEI. The resistance of the SEI is initially comparable with that found for $Li_4Ti_5O_{12}$, namely of the order of 100–200 Ω, to then abruptly increase after aging for 25 cycles, indicating a sudden, massive growth of the surface passivating layer, see Fig. 9b. Since operating well within the electrochemical window of the 0.2 m LiTFSI–Py_{24}TFSI solution (compare Figs. 1a and 8), the $LiFePO_4$ electrodes should be stable in the potential range here examined. Then, the sudden growth of the surface layer is likely due to be associated with external effects, such as precipitation of by-products resulting from reactions at the lithium electrode side.

We have prepared and tested a symmetrical, lithium-free cell formed by two twin $LiFePO_4$ electrodes in their reduced state at ~3 V vs. Li. Fig. 10a shows the impedance response of this cell. The data were obtained at progressive storage times for a total of 38 days. Similar to the $Li_4Ti_5O_{12}$ case, the Nyquist plots evolve with a convoluted semicircle at high frequency, ascribable to the presence of a SEI, followed by a linear behaviour typical of blocking conditions. This result confirms that also the $LiFePO_4$ electrode experiences the formation of a surface passivating layer, SEI, when placed in contact with the 0.2 m LiTFSI–Py_{24}TFSI solution. Importantly, the resistance of this layer is quite low, i.e. of the order of 60–80 Ω, although it tends to slowly and gradually increase upon storage.

Following the protocol used for the $Li_4Ti_5O_{12}$ electrodes, a second symmetrical $LiFePO_4$/$LiFePO_4$ short-circuited cell was assembled with the addition of a third, lithium sink electrode, in this case $Li_4Ti_5O_{12}$. By passing current trough the cell, the $LiFePO_4$ electrodes were brought to a half-discharged state, namely at the

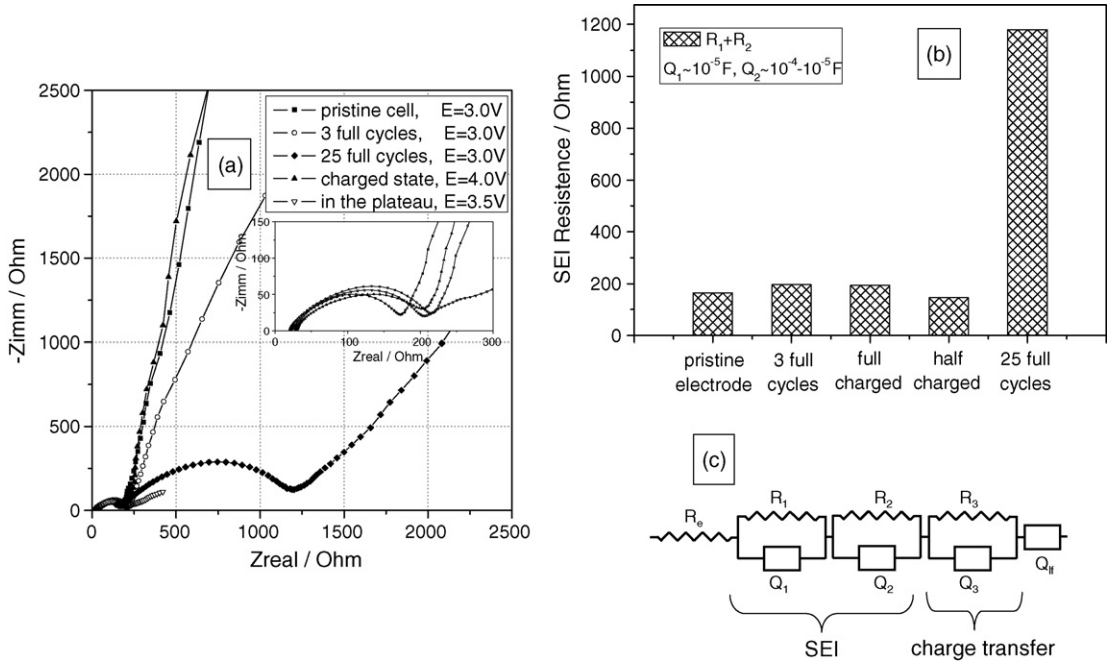

Fig. 9. Impedance response of a $LiFePO_4$ electrode in a 0.2 m LiTFSI–Py_{24}TFSI solution under various stages of the electrochemical process. (a) Nyquist plots; (b) values of the interface resistance; (c) equivalent circuit. Li counter and reference electrodes.

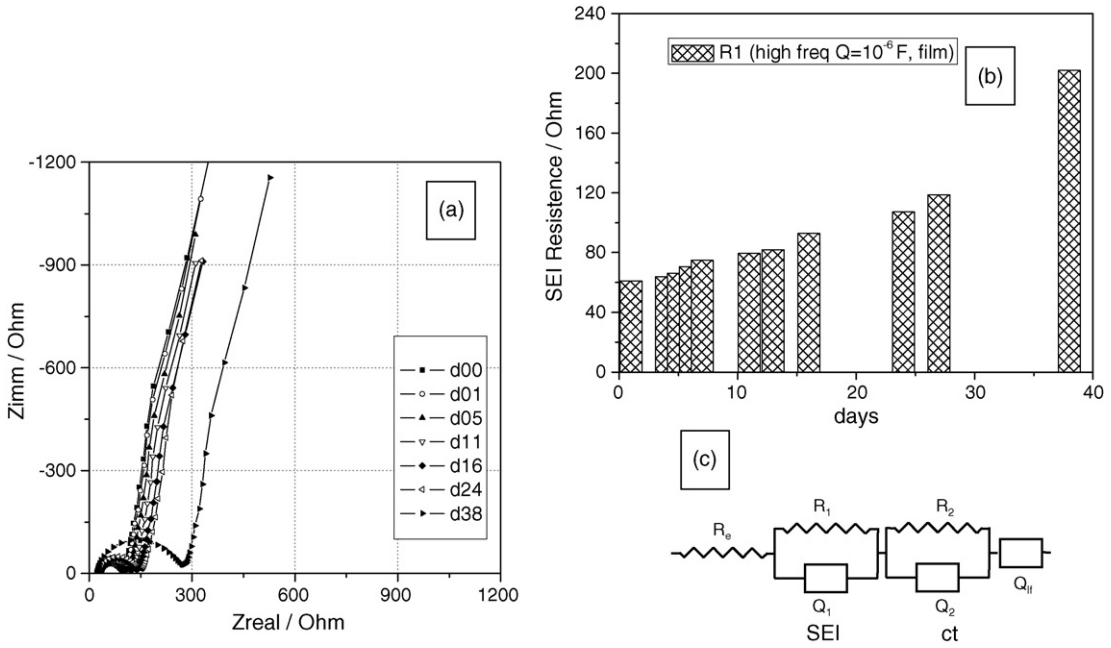

Fig. 10. Impedance response of a symmetrical, lithium-free cell formed by two $LiFePO_4$ twin electrodes in their charged state, i.e. at ~4 V vs. Li, in a 0.2 m LiTFSI–Py_{24}TFSI solution. (a) Nyquist plots at various storage times: d00 means on assembly, d01 means after 1 day, d05 after 5 days and so on; (b) time evolution of the interface resistance; (c) equivalent circuit.

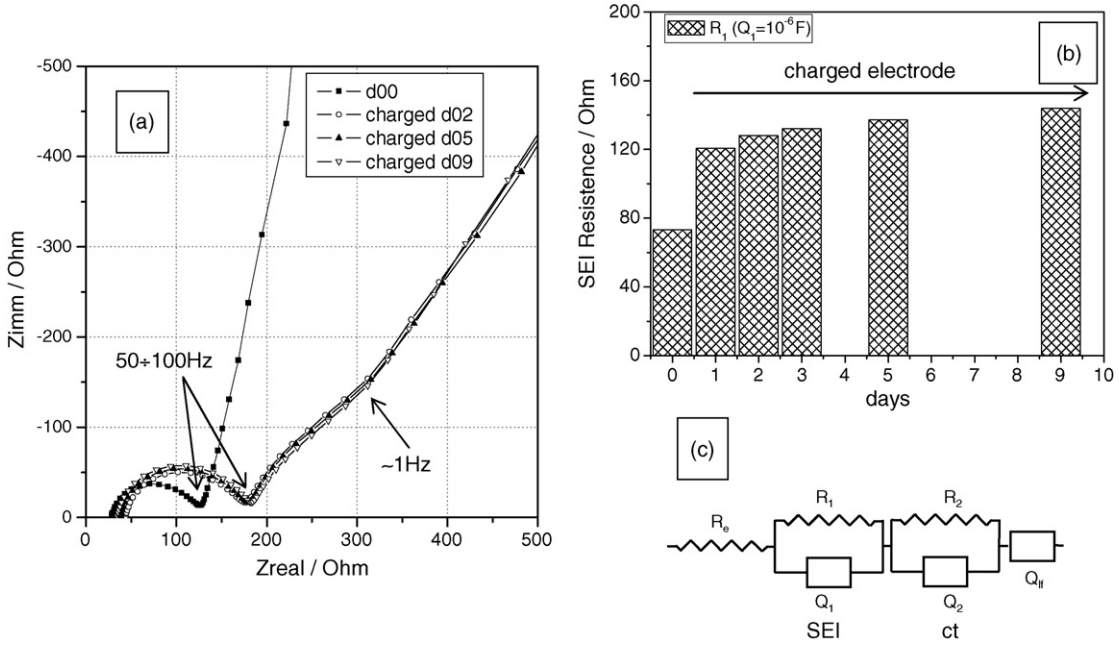

Fig. 11. Impedance response of a symmetrical, lithium-free cell formed by two twin $LiFePO_4$ electrode plus a third, lithium sink $Li_4Ti_5O_{12}$ electrode, in a 0.2 m LiTFSI–Py_{24}TFSI solution. (a) Nyquist plots in the pristine state and after half-discharge; (b) time evolution of the interface resistance; (c) equivalent circuit.

middle of the plateau around 3.4 V vs. Li (compare Fig. 8). The impedance response of this lithium metal-free cell, is shown in Fig. 11a. The effects associated to the SEI surface layer and to the charge transfer resistance (compare discussion of Fig. 6), are easily distinguishable in the high frequency region of the Nyquist plots. Quite interestingly, both the values of these parameters do not change by the time of storage, this finally demonstrating that, as $Li_4Ti_5O_{12}$, also $LiFePO_4$ is a very stable electrode in the IL-based solution examined in this work, but, quite likely, also in the majority of the IL-based solution presently considered for lithium battery application.

4. Conclusion

In this paper we show that IL-based solutions, here exemplified with a 0.2 m LiTFSI solution in Py_{24}TFSI, have a wide anodic stability window, i.e. extending to about 4.5 V vs. Li, while the cathodic window is apparently limited to about 1.5 V vs. Li, probably because of reduction of the IL cation. However, we also show that the initial decomposition results in the formation of a passivation layer on the electrode surface which can be addressed as a solid electrolyte interface, SEI. The SEI occurrence promotes a consistent extension of the cathodic stability.

Passivation with SEI formation is then a key effect in regulating electrode processes in IL-based solutions; it has then appeared to us of interest to carry out a detailed interfacial study of two sample electrodes, both of relevant importance in the lithium ion battery technology, such as a $Li_4Ti_5O_{12}$ anode and a $LiFePO_4$ cathode, in a sample, IL-based, 0.2 m LiTiFSI–Py_{24}TFSI solution. By impedance analysis carried out under different operating condition, we show that a SEI film forms on both electrodes. However, the SEI resistance is low, this being a sign of low thickness, and it does not consistently increases with time, this being a sign of high stability.

These favourable interfacial properties are expected to reflect in a good electrode behaviour and, accordingly, the $Li_4Ti_5O_{12}$–$LiFePO_4$ electrode combination appears very promising for the development of safe, reliable and long-lasting, IL-based lithium ion batteries. Work is in progress in our laboratory to confirm this expectation.

Acknowledgements

This work has been carried out with the financial support of the Italian Ministry of University and Research, MIUR, under a PRIN 2007 project. The authors would like also to thank Prof. Fausto Croce University of Chieti “D’Annunzio” and Prof. Stefania Panero, University of Rome “Sapienza”, for fruitful discussions.

References

[1] H. Ohno, Electrochemical Aspects of Ionic Liquids, Wiley, New York, 2005.
[2] F. Endres, D. MacFarlane, A. Abbott, Electrodeposition From Ionic Liquids, Wiley, New York, 2008.
[3] A. Fernicola, B. Scrosati, H. Ohno, Ionics 12 (2006) 95.
[4] H. Sakaebe, H. Matsumoto, K. Tatsumi, J. Power Sources 146 (2005) 693.
[5] J.-H. Shin, W.A. Henderson, S. Scaccia, P.P. Prosini, S. Passerini, J. Power Sources 156 (2006) 560.
[6] M. Egashira, S. Okada, J. Yamaki, D.A. Dru, F. Bonadies, B. Scrosati, J. Power Sources 138 (2004) 240.
[7] P. Bonhöte, A.-P. Dias, N. Papageogiou, K. Kalyanasundaram, M. Grätzel, Inorg. Chem. 35 (1996) 1168.
[8] D.R. MacFarlane, S.A. Forsyth, J. Golding, G.B. Deacon, Green Chem. 4 (2002) 444.
[9] A. Fernicola, F. Croce, B. Scrosati, T. Watanabe, H. Ohno, J. Power Sources 174 (2007) 342.
[10] D.R. MacFarlane, P. Meakin, J. Sun, N. Amini, M. Forsyth, J. Phys. Chem. B 103 (1999) 4164.
[11] P.C. Howlett, D.R. MacFarlane, A. Hollenkamp, Electrochem. Solid-State Lett. 7 (2004) A97.
[12] S. Panero, P. Reale, F. Ronci, B. Scrosati, V. Rossi Albertini, P. Perfetti, Phys. Chem. Chem. Phys. 3 (2001) 845.
[13] G. Arnold, J. Garche, R. Hemmer, S. Strobele, C. Vogler, M. Wohlfahrt-Mehrens, J. Power Sources 119–121 (2003) 247.
[14] (a) B.A. Boukamp, Solid State Ionics 18 (1986) 136;
(b) B.A. Boukamp, Solid State Ionics 20 (1986) 31.
[15] P. Reale, S. Panero, B. Scrosati, J. Garche, M. Wohlfahrt-Mehrens, M. Wachtler, J. Electrochem. Soc. 151 (12) (2004) A2138–A2142.